Valence XPS, IR, and C13 NMR spectral analysis of 6 polymers by quantum chemical calculations

Valence XPS, IR, and C13 NMR Spectral analysis of 6 polymers by quantum chemical calculations

Kazunaka Endo,* Tomonori Ida,[a] Shingo Shimada,[a] Joseph Vincent Ortiz,[b]
Kenzo Deguchi,[c] Tadashi Shimizu,[c] Kazuhiko Yamada[d]

Center for Colloid and Interface Science, Tokyo University of Science 1-3, Kagurazaka, Shinjuku-ku 162-8601, Japan, [a]Laboratory of Theoretical Chemistry, Graduate School of Natural Science and Technology, Kanazawa University, Kanazawa 920-1192, Japan, [b]Department of Chemistry and Biochemistry, Auburn University, Auburn AL 36849-5312 U. S. A, [c]National Institute for Material Science, 3-13 Sakura, Tsukuba 305-003, Japan, [d]Department of Chemistry and Materials Science, Tokyo Institute Of Technology, 2-12-1-E4-5 Ookayama, Meguro, Tokyo, 152-8552 JAPAN

Valence XPS (VXPS), IR, and C13 NMR spectra of 6 polymers (PE, PS, PMMA, PET, Nylon6, PVC) have been analyzed using the model oligomers from B3LYP/6-31+G(d, p) basis calculations in GAUSSIAN 09. We simulated VXPS of the polymers by the negative of the orbital energies of the ground electronic state at the geometry-optimization of the model oligomers. The simulated VXPS spectra by B3LYP/6-31+G(d, p) basis level were compared with simulated spectra by calculations of SAOP method of ADF program. Simulated IR, and C13 NMR spectra of polymers were obtained from the other SCF calculations of B3LYP/6-31+G(d, p) basis using atomic coordinates of the model molecules at the geometry optimization, in order to gain the vibrational frequencies and nuclear magnetic shielding tensors, respectively. We have clarified the electronic states of the polymers from the good accordance of simulated VXPS, IR, and C13 NMR spectra of polymer models molecules with the experimental ones of the polymers.

Keywords: VXPS, C13-Solid HR-NMR, IR, Polymers

* Corresponding author; Kazunaka ENDO,
e-mail: endo-kz@nifty.com

Introduction

Organic polymers are widely used in diverse applications such as electronics, catalysis, biotechnology, and space science. Such polymer films were obtained by high-performance analytical instruments (X-ray photoelectron spectroscopy (XPS), infrared (IR), nuclear magnetic resonance (NMR), and so on), in order to provide the information on the electronic properties. From a fundamental standpoint as well as for designing materials, it is often important to obtain the electronic states of the polymers. The XPS, IR, and NMR spectroscopy are powerful tools for providing direct information about the density of electronic states. The experimental spectra of polymers can often be directly linked to the calculated electronic density of states as obtained by MO calculations. Since one key feature of polymers is the repetition of the same units, one often uses model oligomers in calculations.

For XPS and X-ray emission spectroscopy (XES), much work was dedicated to such spectroscopy of oligomers and polymers [1-5]. We also used DFT calculations of the model molecules [6-8] with the work, and compare them to experimental XPS and the non-resonant XES of C-, N-, O-, Si-, and S-containing polymers. The comparison of the valence XPS and light element Kα XES with our simulations allowed to distinguish individual contributions for pσ-, pπ-, and nonbonding MOs in the observed valence electron distribution of the polymers.

In this decade, the software performance of the quantum chemical calculation developed remarkably with rapid progress of the hardware capacity of the computer, and we are, then, able to perform the considerable precise calculation about the electronic state of the substances. In the present work, we, thus, intend to predict valence XPS (VXPS), IR and C13NMR spectra of representative polymers (polyethylene (PE), polystyrene (PS), polymethyl methacrylate (PMMA), polyethylene terephthalate (PET), nylon 6 (N6), and polyvinyl chloride (PVC)) from the latest quantum chemical calculation using the polymer model molecules. Definitely, such spectral simulations of the polymers are performed by B3LYP/6-31+G(d,p) basis calculations in GAUSSIAN 09 [9], and we compare the simulated spectra with the experimental results in order to discuss the electronic states of the polymers. Especially, the simulated VXPS spectra by B3LYP/6-31+G(d,p) basis level were compared with simulated VXPS results by calculations of the statistical average of orbital potential

(SAOP) method [10] of Amsterdam density functional (ADF) program [11].

Computational Details

The 1st geometric structures of H-$(CH_2$-$CH_2)_{10}$-H, H-$\{CH_2$-$CH(C_6H_5)\}_3$-H, H-$\{CH_2$-$C(CH_3)COOCH_3\}_3$-H, H-$(OCOC_6H_4COOCH_2CH_2)_2$-H, H-$\{CH_2(CH_2)_3CH_2$-$CONH\}_3$-H, and H-$(CH_2CHCl)_8$-H for PE, PS, PMMA, PET, N6, and PVC polymer model molecules, respectively, were optimized at the AM1 method of Winmopac software [12]. For the 2nd geometry-optimization, we selected the hybrid density functional theory, which was Becke's three parameter hybrid functional [13] with Lee, Yang and Parr's correlation functional [14] (B3LYP), using 6-31+G(d,p) bases in GAUSSIAN 09 software, since the method enables us to obtain a considerable precise energy level with a reasonable computational time, as compared with other precise energy numerations [15]. Then, we performed the 2nd geometry-optimization of the models at the B3LYP/6-31+G(d,p) level. In order to reflect the polymer structural property, we omitted the contribution terms to VXPS, IR, and C13 chemical shielding tensors of both end groups for the 6 polymer models. For the simulated VXPS spectra by the B3LYP/6-31+G(d,p) level, we compared the simulated VXPS spectra of the 6 polymer model molecules by using the SAOP method to obtain reliable vertical ionization potentials (VIP)s in the ADF program.

a) Valence XPS simulation

We simulated VXPS of 6 polymers by using eigenvector coefficients and the negative of the MO eigenvalues for the ground electronic state at the geometry-optimization of the model oligomers at the B3LYP/6-31+G(d,p) level in GAUSSIAN 09. In comparison of the VXPS simulation with the SAOP method in ADF program, the 2nd geometry-optimization of the 6 polymer models was performed with the program. We calculated VXPS spectra of the polymer model oligomers by using the SAOP method to obtain reliable VIPs in the ADF program. The V_{xc}^{SAOP} potential is a statistically weighted interpolation scheme connecting the GLLB V_{xc}^{GLLB} potential [16,17] to the modified LB $V_{\mathrm{xc}}^{LB\alpha}$ potential [18,19]. The V_{xc}^{GLLB} potential is an excellent model

of the exchange-correlation V_{xc} in the core and inner-valence region, capable of reproducing the atomic shell structure. The LB potential excels in the outer-valence region and can reproduce the correct long-range Coulomb asymptote of V_{xc}. Statistical averaging makes the resulting V_{xc}^{SAOP} potential well balanced in all regions. Then, the negative of the orbital energy from a DFT calculation with V_{xc}^{SAOP} approximates the VIPs of outer-valence electrons surprisingly well, in a Koopmans-like manner [20].

1) Solid-state effect

In order to account and somewhat quantify solid-state effects in the polymers under investigation, we considered the difference *WD*, (as described in previous papers [21]) between experimental or theoretical electron binding energy (I_c, or I_k) of model molecules, and the experimental binding energy of the polymers. In order to compare the calculated binding energy for free single molecules in the cluster model and the experimental binding energy of solid polymers, one has to shift each computed value (I_c or I_k) by a quantity *WD* as $I'_c(= I_c - WD)$ {or $I'_k(= I_k - WD)$}, to convert to I'_c (or I'_k) on a common binding energy axis (relative to the Fermi level).

2) Vertical ionization potentials

Vertical ionization potentials were obtained from the negative of the orbital energy for the ground electronic state at the geometry-optimization of the model oligomers at the B3LYP/6-31+G(d,p) level in GAUSSIAN 09, as considered with the Koopmans theorem-like method.

3) Intensity of XPS

The intensity of VXPS was estimated from the relative photoionization cross-section for Al Kα radiation using the Gelius intensity model [22]. For the relative atomic photoionization cross-section, we used the theoretical values from Yeh [23]. In the intensity calculations, we used the LCAO coefficients of eigenvetors for the ground state of the model molecules derived by using a minimal basis set.

To simulate the VXPS, we started with a superposition of peaks centered on each VIP. As described previously [21], each peak is represented by a Gaussian-lineshaped curve. In the case of the linewidth ($WH(k)$), we used $WH(k) = 0.10\ I_k$ (proportional to the ionization energy) for VXPS.

b) IR spectral simulation

Simulated IR spectra of the polymers were obtained from the other SCF calculations of B3LYP/6-31+G(d,p) basis using coordination of the model molecules for 6 polymers at the 2nd geometry-optimization. In order to take into account the calculation of vibrational frequencies, one uses the scaling factor for the calculated frequencies. We used the scaling factor as 0.9614 in the calculations of vibrational frequencies at B3LYP/6-31+G(d,p) level, as Scott and Radom [24] showed.

c) C13 NMR spectral simulation

Simulated C13 NMR spectra of polymers were also obtained from the other SCF calculations of B3LYP/6-31+G(d,p) basis using coordination of the model molecules at the 2nd geometry optimization, because we obtained a better assignment for C13 NMR chemical shielding of methane hydrate from calculations of B3LYP/6-31+G(d,p) basis level [25]. Then, we are able to gain the reasonable results for the nuclear magnetic shielding tensors of polymer model oligomers.

For the ^{13}C NMR chemical shieldings of 6 polymers, the chemical shielding tensors were calculated in the coupled perturbed Hatree-Fock (CPHF) method with the gauge invariant atomic orbital (GIAO) [26]. The calculated chemical shift for ^{13}C is defined by

$$\Delta\sigma = \sigma_{quest} - \sigma_{ref} , \quad (1)$$

where σ_{quest} and σ_{ref} are the chemical shieldings in question and the reference, respectively. The calculated chemical shift is given relative to the reference, tetramethylsilane (TMS). For TMS, we also used the B3LYP/6-31+G(d,p) level calculation, and calculated the shielding constants in the CPHF method with the GIAO.

To simulate solid high-resolution C13 NMR spectra of 6 model molecules, we started with a superposition of peaks centered on each C13 NMR shift of the model molecules. Each peak was represented by a Gaussian-shaped curve. In the case of the line width (WH(k)), we used WH(k) = 2 ppm for C13 NMR shift, in order to simulate the C13 NMR spectrum of model oligomers.

All calculations were performed by ab initio hybrid calculations in GAUSSIAN 09 program on a Panasonic CF-N9 note personal computer.

Experimental

In order to measure the solid C13 cross-polarization (CP) magic angle spinning

(MAS) NMR spectra of 6 polymers, we used the polymer samples {high-density (HD) PE (Prime Polymer Co., Ltd.), PS (Asahi Kasei Chemicals Corp.), PMMA (Sumitomo chemical Co., Ltd.), (PET, and N6) (Mitsubishi Chemical Corp.), PVC(Tosoh Corp.)} furnished from polymer production makers.

The measurement of the C13 CP MAS NMR was performed at frequency of 125.7MHz with JEOL JNM-ECA500 in National Institute for Material Science. We adjusted the CP MAS NMR measurements with the contact time (2 ms) of cross polarization, the MAS of 15 kHz, and the pulse-delay of 5 s, respectively.

We cited the experimental valence X-ray photoelectron spectra [27], and, IR spectra [28] of 6 polymers, respectively. Especially, we cited the C13 solid high-resolution spectra [29, 30] of nylon6 and PS polymers for C13 NMR spectral simulation.

Results and Discussion

We already performed the detailed analysis for valence XPS of more than 60 polymers by DFT calculations using the model molecules [21, 31]. In this section, we aim to simulate VXPS, IR, and C13 CP MAS NMR spectra of PE, PS, PMMA, PET, N6, and PVC polymers using the model oligomers by B3LYP/6-31+G(d,p) basis calculations in GAUSSIAN 09 and to secondly clarify the electronic states of valence XPS, IR, and C13 CP MAS NMR spectra for the polymers.

a) Valence XPS of 6 polymer

In Fig. 1 (a)-(e), valence photoelectron spectra reflect the differences in the chemical structures between 6 polymers (PE, PS, PMMA, PET, N6, PVC). For the valence band XPS spectra in Fig. 1 (a) to (e), the calculated spectra with the B3LYP/6-31+G(d,p) level in GAUSSIAN 9 and the SAOP method in ADF program, respectively correspond well to the experimental ones, although we did not tabulate the parameters (calculated VIPs, main AO photoionization cross-section, orbital nature and functional groups) of their corresponding peaks except for PE, and PMMA polymers, since these were already subject to previous works. It can be predicted from the present MO results that VXPS spectra of the polymers by B3LYP/6-31+G(d,p) level reflect the electronic state at the ground state of each polymer due to the good accordance of simulated spectra with the experimental results.

In a comparison of experimental spectra with simulated results with

B3LYP/6-31+G(d,p) level for PE and PS in Fig. 1 (a) and (b), the simulated spectra of both polymers in the range of 10 – 23 eV show good agreement with the experimental ones, while simulation spectra between 5 and 10 eV are considerably less intensity than experimental ones. The reason of the less intensity is due to the small value of the photoionization cross-section of C2p electron (0.0323 in relative to 1.00 of the C2s electron), although it is partially owing to the populations of C2p atomic orbital in PE and PS model molecules. For the electronic state of PE, we showed the parameters (calculated VIPs, main AO photoionization cross-section, orbital nature and functional groups) of the corresponding peaks in Table 1. However the parameters for PS were omitted, since such datum was already subject to previous work [32].

For PMMA and PET in Fig. 1 (c) and (d), calculated valence photoelectron spectra of the polymer model molecules in GAUSSIAN and ADF programs, respectively are in better accordance than the results in the previous work [21] with the experimental ones. In the figure, the valence electron spectra intensity of both polymers in the ranges of 20-30 and 3-15 eV is due to the main contribution of O2s and O2p photoionization cross-section, respectively. On the other hand, the peaks in the range of 15-20 eV result from C2s photoionization cross-section. In the case of the electronic state of PMMA, we showed the parameters (calculated VIPs, main AO photoionization cross-section, orbital nature and functional groups) of the corresponding peaks in Table 2, although we omit the table for the detailed parameters of the corresponding peaks of the valence spectra for the PET polymer [33].

In the case of N6 polymer in Fig. 1 (e), calculated valence spectra of the model molecules in GAUSSIAN and ADF, respectively are shown and seen to be in considerably good agreement with the experimental spectra. Once again, the detailed table for parameters of the corresponding peaks in valence spectra can be found elsewhere [33]. In the figure, the valence electron peak profile in the ranges of 20-30 and 3-12 eV is owing to the main contribution of (O2s (at around 27 eV), N2s (around 23 eV)) and (O2p, N2p) photoionization cross-section, respectively, while the peak curve in the range of 13-20 eV results from C2s photoionization cross-section.

For PVC in Fig. 1 (f), the intense peak at around 6 eV is due to 3p lone-pair orbitals of pendant Cl of the polymer. Broader spectrum between 15 and 22 eV is determined by Cl 3s main contribution. We, also, omit the table for the detailed parameters of the

corresponding peaks of the valence spectra for the PVC polymer [21].

b) IR spectra of 6 polymers

We used the scaling factor as 0.9614 in the calculations of vibrational frequencies for the 6 polymer model molecules at B3LYP/6-31+G(d,p) level. In Table 3, we showed the calculated C-H stretching frequencies (2900-3000 cm^{-1}) of six model molecules with the experimental values. By considering the stretching and bending vibrations of PE model as the referred vibrations, we are able to see such vibrations of representative functional groups of polymer models (=C-H of PS, (-C=O, -C-O) of PMMA and PET, (-N-H, $-NH_2$,-C=O) of Nylon6, -C-Cl of PVC, respectively).

In Fig. 2 (a)-(e), IR spectra also reflect the differences in the chemical structures between 6 polymers (PE, PS, PMMA, PET, N6, PVC). For IR spectra in Fig. 2 (a) to (e), the simulated spectra correspond well to the experimental ones except for Nylon6 in the figure (e).

c) C13 solid NMR spectra of 6 polymers

1) Correlation between the calculated and experimental solution C13 chemical shifts

Figure 3 (a) – (f) shows the correlation between the present theoretical C13 chemical shifts of PE, PS, PMMA, PET, Nylon6 and PVC polymer model molecules and the experimental solution C13 chemical shifts of the polymers in organic solvents from data packages of NIMS [34]. In the figure, we may conclude that the calculated values are in good correlation with the experimental results.

In tables 4-8, we showed the calculated C-13 chemical shifts of functional groups for the polymer models with the experimental ones for polymers in solution. The calculated results are also in good accordance with experimental values in absolute average deviations of ± 4.42 ppm.

In the tables, calculated shielding constants of all carbons for the polymer models can be reflected the experimental chemical shifts in the 6 polymers. For carbons of PE, PS, PMMA, and PVC polymers, the experimental shifts of the saturated -CH-, $-CH_2$, and $–CH_3$ groups are seen to be determined by the paramagnetic shielding constants, since the diamagnetic shielding constants are almost similar values within 230 - 300 ppm. In the case of PET and N6 polymers involving large electro-negativity O and N atoms, it is interesting that the diamagnetic and paramagnetic shielding terms of all carbons have different values, respectively.

2) Simulation of C13 CP MAS spectra for 6 polymers

In previous section, we showed the good correlation between the calculated shifts of 6 polymer models and the experimental solution C13 chemical shifts of the polymers. Thus, we simulated observed C13 CP MAS NMR spectra of the polymers from the chemical shielding constants of the model oligomers in Fig. 4 a) – f).

In the figure, the simulated spectra are in good accordance with the observed C13 CP MAS results. In the simulated C13 spectra of 6 polymers, we performed detailed spectral analysis of N6 and PS in Fig. 5 a) and b). In the figure, we also referred good resolution CP MAS spectra of the polymers [29, 30]. In the case of N6, the C13 NMR solid high resolution spectra were compared with the calculated C13 spectra plotted with the linewidth of 1 ppm. It is very interesting that chemical shifts of every methylene functional groups in simulated spectra show nice accordance with those of experimental spectra in Fig. 5 a). For PS polymer, calculated chemical shifts of -CH- and -CH_2 functional groups are also in good agreement with experimental ones in Fig. 5 b).

Conclusion

We have analyzed valence XPS (VXPS), IR, and C13 NMR spectra of 6 polymers (PE, PS, PMMA, PET, N6, PVC) by quantum chemical calculations (B3LYP/6-31+G(d,p) basis calculations in GAUSSIAN 09) using the model oligomers. It enabled us to confirm that the simulated VXPS spectra of the polymer models from the negative of orbital energies at B3LYP/6-31+G(d, p) level correspond well to the simulation results from calculations with the SAOP method in ADF software. Then, we could show that VXPS, IR, and C13 NMR spectra of polymer models by B3LYP/6-31+G(d,p) basis calculations are in good agreement with spectral results in VXPS, IR, and C13 CP MAS NMR experiments. We, thus, clarified the electronic states of the polymers from the good accordance of simulated VXPS, IR, and C13 NMR spectra of polymer with the experimental ones.

From these results, it will enable us to predict the identification of VXPS, IR, and C13 NMR spectra of new polymers using quantum chemical calculations in future.

References

[1] J.-H. Guo, M. Magnuson, C. Såthe, J. Nordgren, L. Yang, Y. Luo, H. Ågren, K. Z.Xing, N. Johansson, W. R. Salaneck, R. Daik, W. J. Feast, J. Chem. Phys. **108** (1998)5990.

[2] E. Z. Kurmaev, A. Moewes, J. -C. Pivin, M. Bach, K. Endo, T. Ida, S. Shimada, M. Neumann, S. N. Shamin, D. L. Ederer, M. Iwami, J. Mater. Sci., **37**(2002)3789.

[3] E.Z. Kurmaev, A. Moewes, T. Ida, S. Danielache, K. Endo, I.O. Bashkin, A.I. Kharkunov and A.P. Moravskii, J. Mol. Struct. Theo. Chem. **639**(2003)27.

[4] E.Z. Kurmaev, J. P. Werner, A. Moewes, S. Chiuzbăian, M. Bach, W. –Y. Ching, W. Motozaki, T. Otsuka, S. Matsuya, K. Endo, M. Neumann, J. Electr. Spectr. Relat. Phenom. **137-140**(2004)81.

[5] D. W. Boukhvalo, M. Al-Saqer, E. Z. Kurmaev, A. Moewes,V. R. Galakhov, L. D. Finkelstein, S. Chiuzbaian, M. Neumann, V. V. Dobroviski, M. I. Katsnelson, A. L. Lichtenstein, B. N. Harmon, K. Endo, J. M. North, N. S. Dalal, Phys. Rev. **B75**(2007)014419.

[6] K. Endo, S. Shimada,T. Ida, M. Suhara, E. Z. Kurmaev, A. Moewes, D. P. Chong, J. Mol. Struct. **561**(2001)17.

[7] K. Endo, S. Koizumi, T. Otsuka, T. Ida, T. Morohashi, J. Onoe, and A. Nakao, E. Z. Kurmaev, A.Moewes, D. P. Chong, J. Phys. Chem. **A 107**(2003) 9403.

[8] S. Shimada, T. Hiroi, T. Ida, M. Mizuno, K.Endo, E. Z. Kurmae , A. Moewes, J. Polym. Sci. Part B Polym. Phys. **45**(2007)162.

[9] http://www.gaussian.com/g_prod/g09.htm.

[10] P.R.T. Schipper, O.V. Gritsenko, S.J.A. van Gisbergen, E.J. Baerends, J. Chem. Phys. **112**(2000)1344.

[11] R. Van Leeuwen, E. J. Baerends, Phys. Rev. A **49**(1994)2421.

[12] M. J. S. Dewar; E. G. Dewar, Theochem. **180**(1988)1; M. J. S. Dewar; E. G. Dewar; H. F. Healy; J. J. P. Stewart, J. Am. Chem. Soc. **107**(1985)3902.

[13] A.D. Becke, J. Phys. Chem., **97**(1992)9173.

[14] C. Lee, W. Yang, R.G. Parr, Phys. Rev. **B 37**(1988)785.

[15] J. B. Foresman, AE. Frisch, "Exploring Chemistry With Electronic Structure Methods: A Guide to Using Gaussian," 2nd Edition, Gaussian, Inc. Pittsburgh, Pennsylvania, USA, 1996.

[16] O.V. Gritsenko, R. van Leeuwen, E. van Lenthe, E.J. Baerends, Phys. Rev. A **51**(1995)1944.

[17] O.V. Gritsenko, R. van Leeuwen, E.J. Baerends, Int. J. Quant. Chem. **61**(1997) 231.

[18] P.R.T. Schipper, O.V. Gritsenko, S.J.A. van Gisbergen, E.J. Baerends, J. Chem. Phys. **112**(2000)1344.

[19] R. van Leeuwen, E.J. Baerends, Phys. Rev. A **49** (1994)2421.

[20] D. P. Chong, O.V. Gritsenko, E.J. Baerends, J. Chem. Phys. **116** (2002)1760.

[21] K. Endo, Y. Kaneda, H. Okada, D. P. Chong, P. Duffy, J. Phys. Chem.,**100**(1996)19455; K. Endo, S. Maeda, M. Aida, Polymer J. **29**(1997)171; K. Endo, S. Maeda, Y. Kaneda, Polymer J. **29** (1997)255.

[22] U. Gelius, K. Siegbahn, Faraday Discus. Chem. Soc. **54** (1972)257; U. Gelius, J. Electron. Spectrosc. Relat. Phenom. **5** (1974)985.

[23] J.-J. Yeh, Atomic Calculation of Photoionization Cross-Section and Asymmetry Parameters, Gordonand Breach, NJ, 1993.

[24] Scott A.P., Radom L., J. Phys. Chem., 100(1996)16502.

[25] T. Ida, M. Mizuno, K. Endo, J. Compt. Chem. **23**(2002)1071.

[26] De Dios A.C., Prog. Nucl. Magn. Reson. Spectrosc., 29(1996)229.

[27] G. Beamson, D. Briggs, "High resolution XPS of organic polymers", John Wiley & Sons, Chichester–New York- Brisbane Toronto-Singapore, 1992.

[28] http://www.ir-spectra.com/polymers/NICODOM IR Polymers, FTIR spectra of polymers Copyright © NICODOM 2006-2010

[29] D.L. VanderHart, A. Asano, and J.W. Gilman, Macromolecules, 34, 3819(2001); Chemistry of Materials,13(2001)3781.

[30] A. Grassi, P. Longo, Makromol. Chem. Rapid Commun.. 10(1989)687.

[31] K. Endo, and D. P. Chong, J. Surf. Anal.3(1997)618; 4(1998)50.

[32] M. Aida, Y. Kaneda, N. Kobayashi, K. Endo, D. P. Chong, Bull. Chem. Soc. Jpn., 67 (1994)2972.

[33] K. Endo, C. Inoue, Y. Kaneda, M. Aida, N. Kobayashi, D. P. Chong, Bull. Chem. Soc. Jpn., 68(1995)528.

[34] http://polymer.nims.go.jp/ NMR Database: PoLyInfo.

Highlights

- We intend to predict electron spectra of polymers from quantum chemical calculation using the polymer oligomer models.
- Valence XPS, IR, and C13 NMR spectra of representative polymers are obtained from B3LYP/6-31G** basis calculations in GAUSSIAN 09.
- It enabled us to confirm that the simulated VXPS spectra of the polymer models from the negative of orbital energies at B3LYP/6-31+G(d, p) level correspond well to the simulation results from calculations with the SAOP method in ADF software.
- We clarify the electronic states of the polymers from the good accordance of simulated VXPS, IR, and C13 NMR spectra of polymer models molecules with the experimental ones of the polymers.

Figure(s)

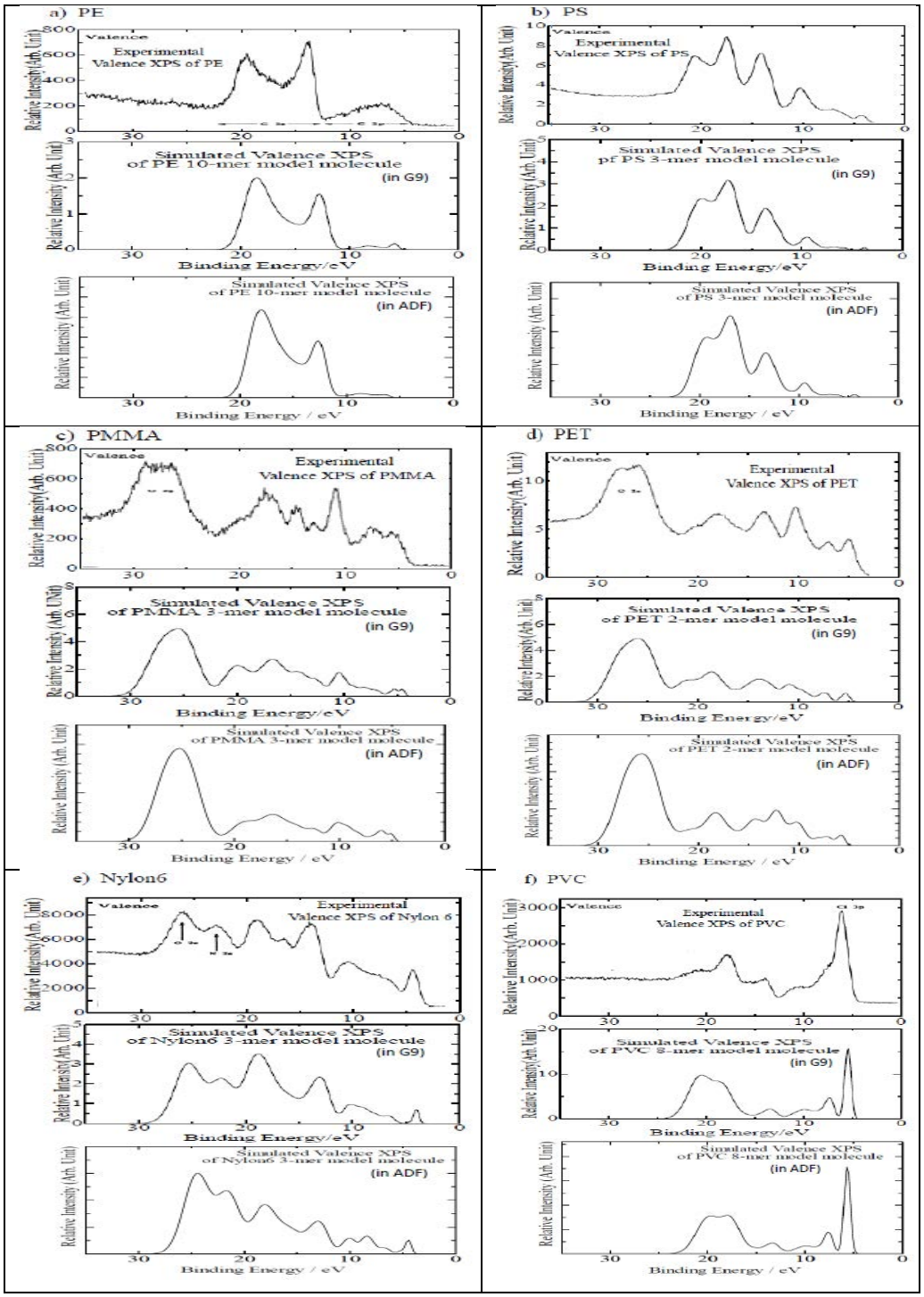

Fig.1 Valence XPS of 6 polymers (upper: experimental, middle: simulatein G9, lower: simulated in ADF) (a)PE (b)PS (c)PMMA (d)PET (e)N6 (f)PVC

Figure(s)

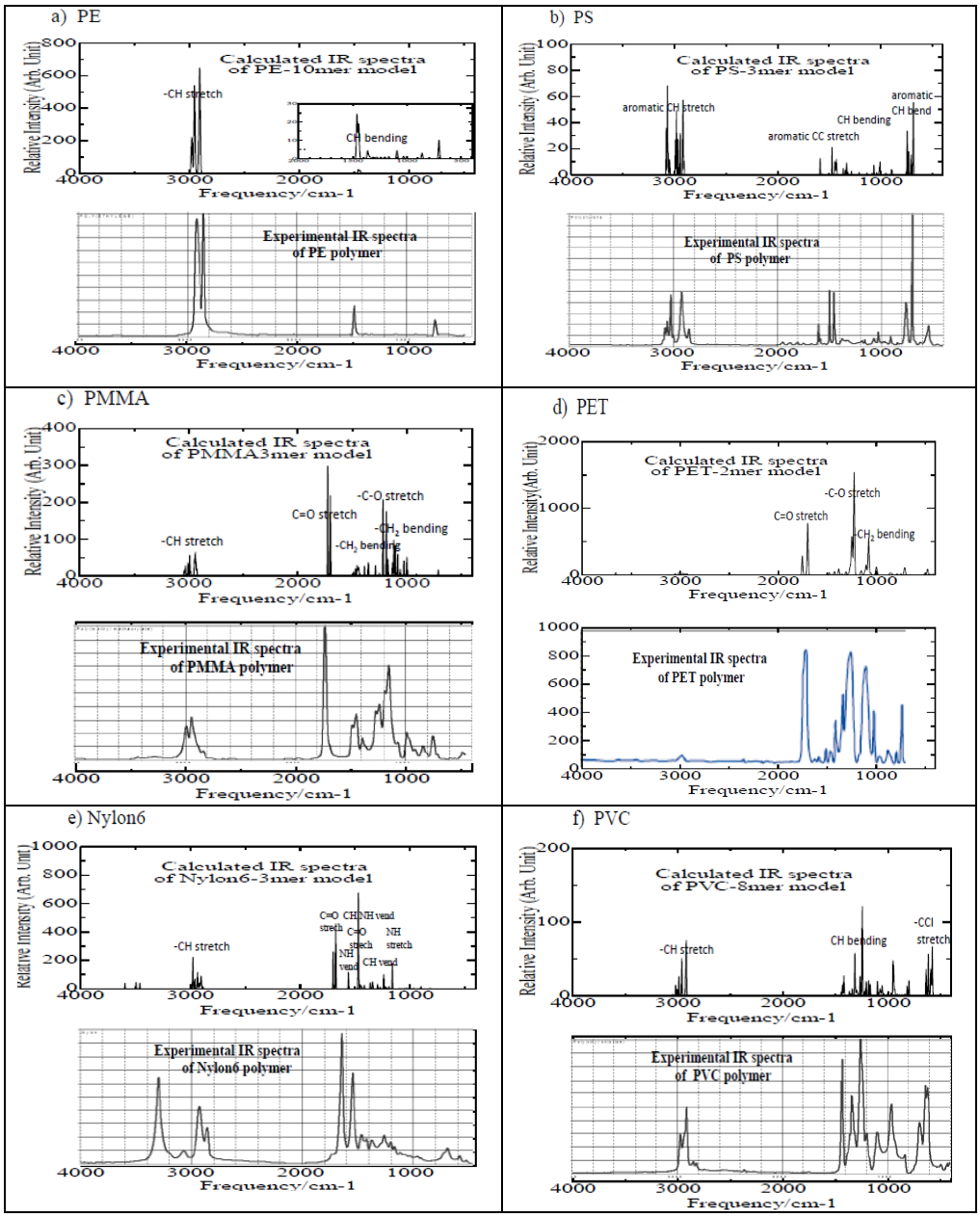

Fig.2. IR spectra of 6 polymers (upper: simulated, lower: experimental)
(a)PE(b)PS(c)PMMA(d)PET(e)N6(f)PVC

Figure(s)

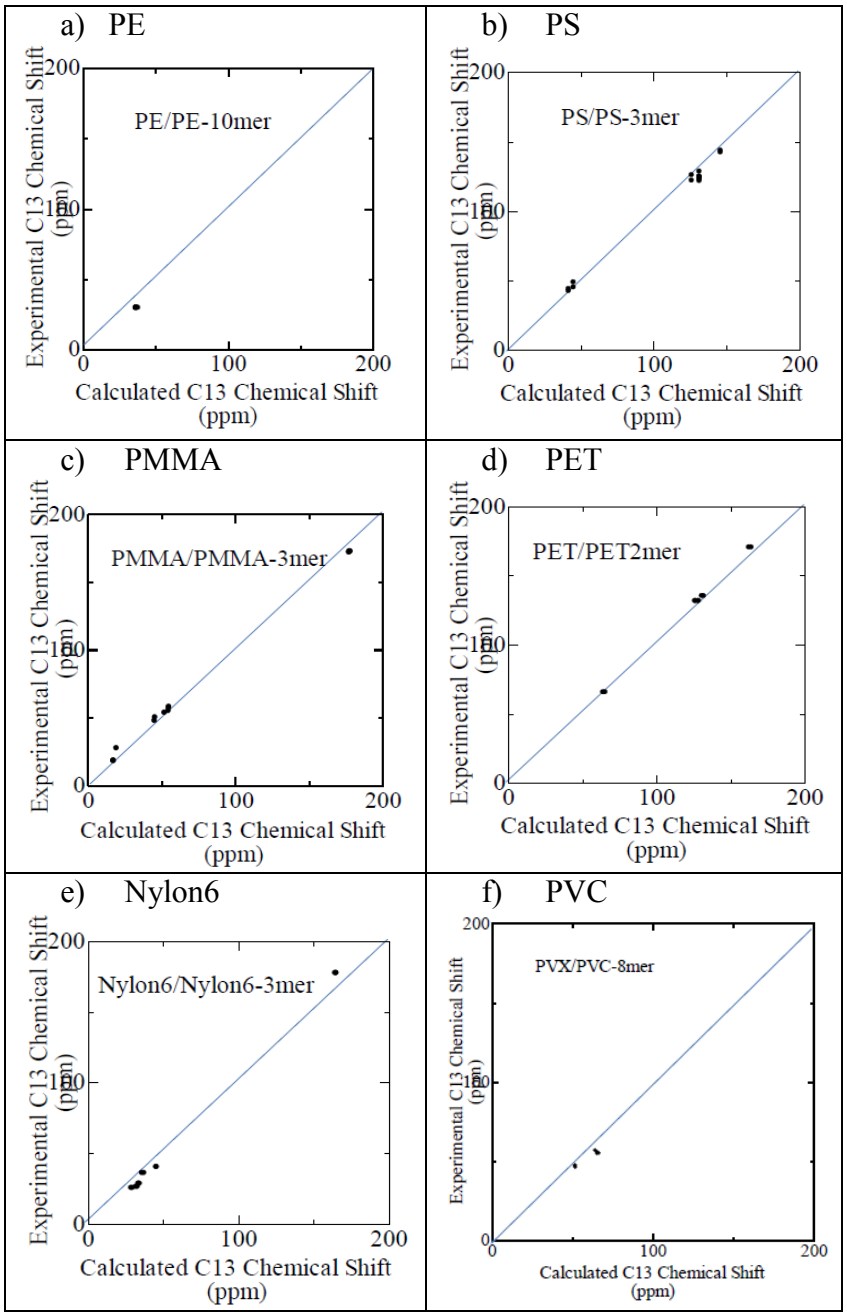

Fig.3. Comparison between experimental solution and calculated values for the C13 chemical shifts of 6 polymers ((a)PE (b)PS(c)PMMA(d)PET(e)N6(f)PVC).

Figure(s)

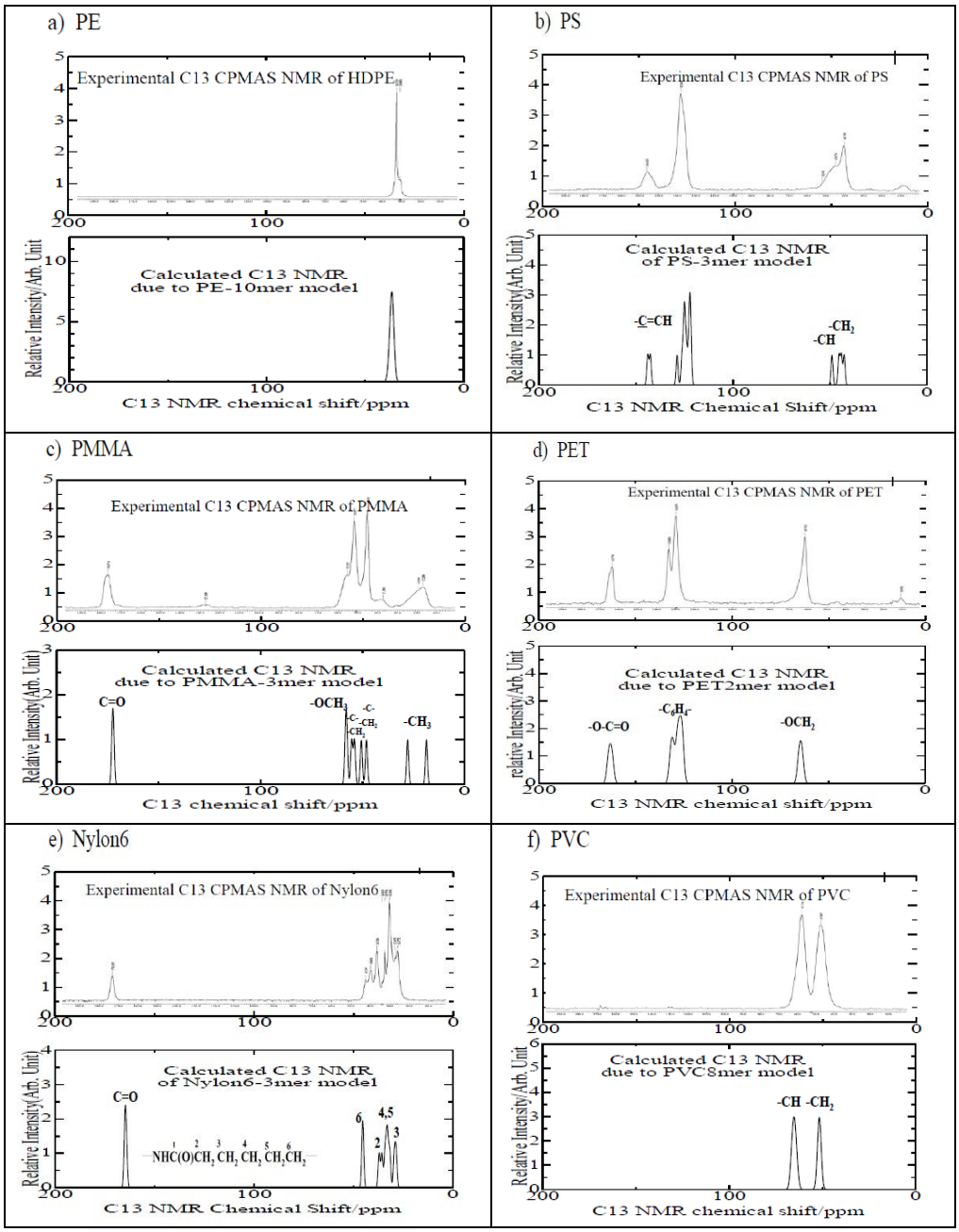

Fig.4. C13 solid HR NMR spectra of 6 polymers (upper: experimental, lower: simulated) (a)PE(b)PS(c)PMMA (d)PET(e)N6(f)PVC

Figure(s)

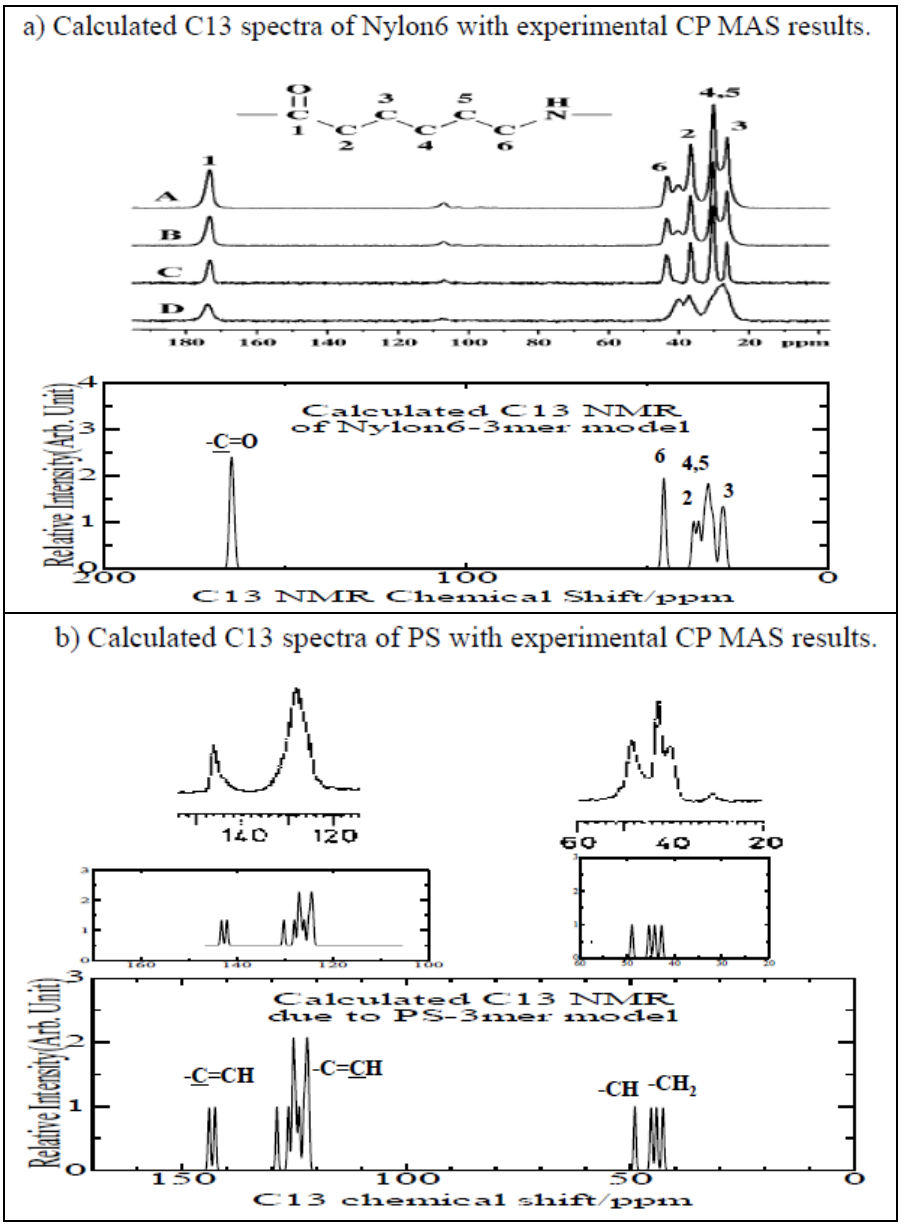

Fig.5. C13 solid HR NMR spectra with simulated ones
(upper: experimental, lower: simulated) (a)N6 and (b) PS

Table(s)

Table 1. Observed peak, VIP, main AO photo-ionization cross-section, orbital nature and functional group for Valence XPS of PE

observed peak (eV)	VIP (eV)	main AO photo-ionization cross-section	orbital nature[b]	functional group
19.0(22.0-17.0)[a]	22.21-18.51	C2s	sσ(C2s-C2s)-B	-C(main chain)
13.5(17.0-12.0)[a]	17.82-15.48	C2s	s, pσ(C2s-C2s,p)-B	-C(main chain)
7.5(12.0-4.0)[a]	13.29-10.44	C2p	pσ(C2p-C2p)-B	-C(main chain)
	10.32-7.82	C2p	pσ (C2p-H1s)-B	-CH

[a] shows the peak range.
[b] B and NB mean bonding and nonbonding, respectively.

Table 2. Observed peaks, VIP, main AO photo-ionization cross-section, orbitals nature and functional group for valence XPS of PMMA

observed peak (eV)	VIP (eV)	main AO photo-ionization cross-section	orbital nature[b]	functional group
27.0(30.0-22.0)[a]	30.43-27.77	O2s(0.9), C2s(0.1)	sσ(O2s-C2s)-B	-O-, O=C
		O2s	pσ(O2s-C2s)-B	-O-, O=C
18.0(22.0-16.0)[a]	23.36-18.98	C2s	pσ(O2p-C2s)-B	O=C
		C2s	sσ(C2s-C2s)-B	C-C (main chain)
15.0(16.0-14.0)[a]	18.08-15.80	C2s (0.9), O2s(0.1)	sσ(C2s-C,O2s)-B	-C-C, -O-CH_3
13.0(14.0-12.0)[a]	15.56- 14.60	O2p, C2s, O2s	pσ(O, C2p-C2s)-B	-O-C-C, O=C-C
11.0(12.0-10.0)[a]	14.20-12.10	O2s(0.5), O2p, C2s	pσ(O,C2p-O,C2s)-B	-O-CH_3
8.0(10.0-7.0)[a]	12.01-9.48	O2p, C2p	pσ, pπ(O,C2p-2p)-B	-C-C-O, O=C-C
5.0(7.0-3.0)[a]	9.06-7.45	O2p	pπ(lone-pair)-NB	O=C, -O-C

[a] shows the peak range.
[b] B and NB mean bonding and nonbonding, respectively.

Table 3. Calculated IR frequencies of polymer models with experimental ones of polymers

streching vibrations			bending vibrations		
functional group	model molecule range(cm^{-1})	**experimental** range(cm^{-1})	functinal group	model molecule range(cm^{-1})	**experimental** range(cm^{-1})
-CH, $-CH_2$	PE (2904,2952, 2975)	**2850-3000**	$-CH_2$	PE (1445, 1461)	**1450-1500**
				PE (706)	**720-725**
-CH, $-CH_2$	PS(2915, 2918, 2945, 2965, 2981, 2991)	**2850-3000**	$-CH_2$	PS (1432, 1472)	**1420-1470**
			-CH	PS (705,730,743)	**750-800**
=C-H	PS(3061, 3068, 3080)	**3020-3100**	=C-H	PS(1006, 1012)	**1050-1100**
-C-C	PS(1588)	**1580-1600**			
-CH, $-CH_2$, $-CH_3$	PMMA (2925,2933,2938, 2944,2947, 2990)	**2850-3050**	$-CH_2$	PMMA (1350,1353, 1386, 1439,1445,1454,1469)	**1350-1470**
-C=O	PMMA (1699, 1724)	**1700-1750**	$-CH_2$	PMMA(710)	**720-770**
-C-O	PMMA (998,1025, 1082, 1105,11171186, 1217)	**970-1300**			
-CH, $-CH_2$	PET(2932,2950.2969, 2976,3001,3013)	**2950-3050**	$-CH_2$	PET (705,713)	**720-750**
-C=O	PET (1698,1702,1754)	**1700-1800**	-		
-C-O	PET (1077, 1103,1115,1151, 1225,1244,1252, 1268)	**1000-1300**			
-NH	Nylon6(3459,3493,3494)	**3400-3500**	CH_2	Nylon6(1295,1342, 1363,1454,)	**1350-1450**
-CH, $-CH_2$	Nylon6(2898,2904,2912 2921,2933,2935,2958,2976)	**2850-3000**	$-NH_2$, CH_2	Nylon6(1469,1471 , 1474,1560)	**1500-1600**
-C=O	Nylon6 (1676,1699)	**1600-1850**	CH_2, $-NH_2$	Nylon6(1161,1239)	**1200-1300**
-CH, $-CH_2$	PVC (2920,2926, 2962,2990)	**2850-3000**	$-CH_2$	PVC (1316, 1340,1420, 1432,1435)	**1350-1470**
-CC	PVC(800,818,946,,952, 1055,1100, 1169,1184,1207,1240-1265)	**800-1000**			
-CCl	PVC(638)	**600-750**			
-CC, CCl	PVC(594,617)	**600-750**			
-CC	PVC(579,587)	**600-750**			

Table 4. C13 Magnetic shielding constant (ppm) of PE and PVC

C13NMR of PE and PVC	$-CH_2$ (PE)	-CH(PVC)	$-CH_2$(PVC)	-C13 (TMS)
Experimental values	29.81	57.11;56.13 55.24;55.10	47.92;47.47 47.14;46.38 45.60	0.00
Calculated values	36.34;36.37 36.45;36.41 36.32 ;36.27	64.00; 66.35 65.35	51.78; 51.79 51.49	0.00
Total chemical shielding constants	156.28; 156.25 156.17; 156.21 156.30; 156.35	127.26; 128.62 126.27	140.84; 140.83 141.13	192.62
diamagnetic shielding constants	253.89; 253.39 251.07; 258.41 250.27; 251.84	255.39; 237.91 235.70	241.02; 283.08 259.78	252.95
paramagnetic shielding constants	-97.61; 97.14 -94.90; -102.20 -93.98; -95.49	-126.77;-111.63 -108.44	-100.18;-142.24 -118.65	-60.34

Table 5. C13 Magnetic shielding constant (ppm) of PS

C13NMR of PS	-C(1)=	-C(2)H=	-C(3)H=	-CH-	$-CH_2$	-C13 (TMS)
Experimental values	145.51	131.02	125.75	41.38	44.77	0.00
Calculated values	142.64 143.95	122.79;125.25;123.88 128.83;121.74;125.11 124.67; 126.26	122.48 122.06	45.38 42.72	44.17 48.99	0.00
Total chemical shielding constants	49.98 48.67	69.83; 67.37; 68.74 63.79; 70.88; 67.51 67.95; 66.36	70.32 70.56	147.24 149.90	148.45 143.63	192.62
diamagnetic shielding constants	344.14 330.75	191.17;309.60; 293.43 239.78;226.54; 300.29 283.38; 245.624	219.97 245.61	330.05 289.76	252.35 270.79	252.95
paramagnetic shielding constants	-294.16 -282.07	-121.34; -242.23;-224.69 -175.98; -155.67; -232.79 -215.43; -179.26	-149.65 -175.05	-182.81 -139.86	-103.90 -127.17	-60.34

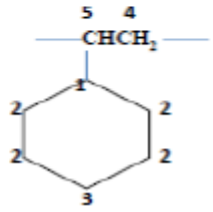

Table 6. C13 Magnetic shielding constant (ppm) of PMMA

C13NMR of PMMA	-O<u>C</u>=O	-<u>C</u>H_2	O-<u>C</u>H_3	-C(4)-	-<u>C</u>H_3	-C13 (TMS)
Experimental values (syndiotactic-)	177.70 177.60 177.11 177.02 176.93	54.73 54.57 54.30	51.69	45.24 44.95	19.09 17.17 17.08 17.03	0.00
Calculated values	172.66 172.10	55.30 50.54	58.25 57.67	53.95 48.04	27.83 18.61	0.00
Total chemical shielding constants	19.96 20.52	137.32 142.08	134.37 134.95	138.67 144.58	164.79 174.01	192.62
diamagnetic shielding constants	242.84 241.06	245.79 255.25	233.85 242.77	298.92 277.53	228.95 237.21	252.95
paramagnetic shielding constants	-222.89 -220.54	-108.47 -113.17	-99.48 -107.82	-160.25 -132.95	-64.16 -63.21	-60.34

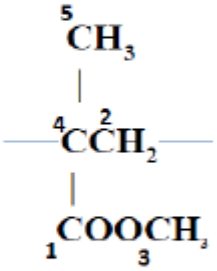

Table 7. C13 Magnetic shielding constant (ppm) of PET

C13NMR of PET	-O<u>C</u>=O	-<u>C</u>(2)=	-<u>C</u>H=	O-CH_2	-C13 (TMS)
Experimental values	170.74	135.63	132.01	66.10	0.00
Calculated values	162.24 163.84	131.69 130.46	125.85;127.68 126.20;128.32	65.21 66.45	0.00
Total chemical shielding constants	30.38 28.78	60.93 62.16	66.77; 64.94 66.42; 64.30	127.41 126.17	192.62
diamagnetic shielding constants	256.90 249.60	253.74 297.12	260.49; 249.54 237.17; 294.85	230.48 232.49	252.95
paramagnetic shielding constants	-226.52 -220.82	-192.80 -234.96	-193.72; -184.60 -170.75; -230.54	-103.07 -106.32	-60.34

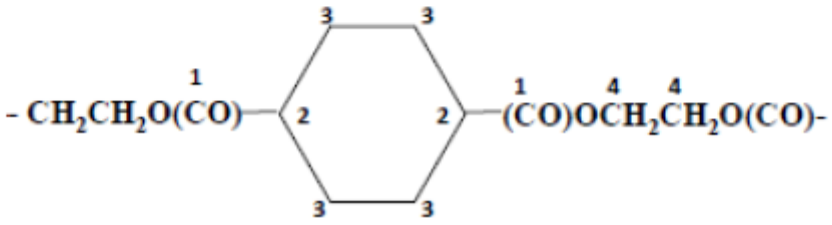

Table 8. C-13 Magnetic shielding constant (ppm) of Nylon6

C13NMR of Nylon6	-C(1)=O	-C(2)-	-C(3)-	-C(4)-	-C(5)-	-C(6)-N	-C13 (TMS)
Experimental values	177.76	36.37	25.81	28.82	26.57	40.63	0.00
Calculated values	164.88 164.13 164.85	37.98 37.09 35.69	29.77 29.40 28.51	31.71 32.71	33.26 34.12	45.19 45.41	0.00
Total chemical shielding constants	27.74 28.49 27.77	154.64 155.53 156.94	162.83 163.22 164.11	160.91 159.91	159.36 158.50	147.43 147.21	192.62
diamagnetic shielding constants	281.90 304.54 266.16	209.67 178.72 217.19	261.12 287.12 263.65	292.38 279.22	198.58 204.62	303.22 291.53	252.95
paramagnetic shielding constants	-254.17 -276.o4 -238.39	-55.03 -23.19 -60.36	-98.29 -123.89 -99.54	-131.47 -119.30	-39.22 -46.12	-155.79 -144.32	-60.34